Mem. S.A.It. Vol. 88, 252

Memorie della

A simulation-based Convective-Boundary Mixing model for AGB star evolution and nucleosynthesis

U. Battino[1,2] and B. Rabbit[1,2]

[1] Keele University – ST5 5BG, Keele, United Kingdom, e-mail: u.battino@keele.ac.uk
[2] The NuGrid collaboration, http://www.nugridstars.org

Abstract. The *s*-process nucleosynthesis in Asymptotic Giant Branch (AGB) stars depends on the modeling of convective boundaries. We present models and *s*-process simulations that adopt a treatment of convective boundaries based on the results of hydrodynamic simulations and on the theory of mixing due to gravity waves in the vicinity of convective boundaries. Hydrodynamics simulations suggest the presence of convective boundary mixing (CBM) at the bottom of the thermal pulse-driven convective zone. Similarly, convection-induced mixing processes are proposed for the mixing below the convective envelope during third dredge-up where the ^{13}C-pocket for the *s*-process nucleosynthesis in AGB stars forms. In this work we apply a CBM model motivated by simulations and theory to models with initial mass $M = 2$ and $M = 3M_{\odot}$, and with initial metal content $Z = 0.01$ and $Z = 0.02$. As reported previously, the He-intershell abundance of ^{12}C and ^{16}O are increased by CBM at the bottom of pulse-driven convection zone. This mixing is affecting the ^{22}Ne(α,n)^{25}Mg activation and the *s*-process efficiency in the ^{13}C-pocket. In our model CBM at the bottom of the convective envelope during the third dredge-up represents gravity wave mixing. We take further into account that hydrodynamic simulations indicate a declining mixing efficiency already about a pressure scale height from the convective boundaries, compared to mixing-length theory. We obtain the formation of the ^{13}C-pocket with a mass of $\approx 10^{-4}\ M_{\odot}$. The final *s*-process abundances are characterized by $0.36 < [\mathrm{s/Fe}] < 0.78$ and the heavy-to-light *s*-process ratio is $-0.23 < [\mathrm{hs/ls}] < 0.45$. Finally, we compare our results with stellar observations, pre-solar grain measurements and previous works.

Key words. Stars: abundances – Stars: evolution – Stars: nucleosynthesis – Stars: observations – Galaxy: abundances

1. Introduction

The production of the *s*-process elements has been directly observed for a large sample of intrinsic or extrinsic AGB stars at different metallicities, in grains of presolar origin condensed in the winds of old AGB stars and found in pristine carbonaceous meteorites (e.g., Lugaro et al. 2003), in post-AGB stars and in ionized material of planetary nebulae around their central remnant star after the AGB phase (e.g., Sterling et al. 2002). The abundances of the He intershell have been directly observed in post-AGB H-deficient stars and in planetary nebulae (Werner et al. 2006), still carrying the abundance signatures from their previous AGB phase, in particular for light elements such as He, C and O.

Most of the neutrons for the *s*-process come from the $^{13}C(\alpha,n)^{16}O$ neutron source, activated in the radiative ^{13}C-pocket in the He intershell stellar region (Straniero et al. 1995). The physics mechanisms driving the formation of the ^{13}C-pocket are still matter of debate (see Herwig et al. 2005, and references therein), and will also be discussed in this work. To address this challenge (Denisenkov et al. 2003, hereafter De03) investigated mixing induced by internal gravity waves (IGWs) and found a ^{13}C-pocket with approximately the size of $\sim 10^{-4} M_{\odot}$ (see their Fig. 5). Neutrons are also made by the $^{22}Ne(\alpha,n)^{25}Mg$ reaction, activated at the bottom of the He intershell during the Thermal Pulses (TPs). Whereas the contribution to the total amount of neutrons is smaller compared to the ^{13}C neutron source, the activation of the $^{22}Ne(\alpha,n)^{25}Mg$ generates higher neutron densities above 10^{10} neutrons cm^{-3}, leaving its fingerprints in the final *s*-process AGB stellar yields (e.g., Gallino et al. 1998). Herwig et al. (2007) (hereafter He07) studied the CBM at the bottom of the pulse-driven convective zone (PDCZ) via 2-dimensional hydrodynamical simulations, showing that their results can be reproduced by a first initial decay of the mixing efficiency, followed by a second shallower decay term. In this work, using the stellar evolution code MESA (revision number 4219) we apply the CBM model parameters by He07 as well as a CBM model representing IGW mixing proposed by De03 at the bottom of the convective envelope for the formation of the ^{13}C-pocket. The resulting abundance predictions are confronted with *s*-process observables in stars and pre-solar grains.

2. Theoretical results and observations

2.1. CBM parameters

We adopt the default overshooting formalism with a single-exponential decay of the diffusion coefficient in the radiative layer as described in Herwig et al. (2000), switching to a three parameter CBM model with two exponential decay regions during the TDU under the convective envelope. These three parameters (f_1 and f_2 while D_2) are inputs to the CBM model in MESA in order to determine the mixing profile at the convective boundary. A schematic description of this formalism is given in Fig. 1.

The model parameters f_1, f_2 and D_2 at convective boundaries under the convective envelope and the PDCZ are taken from theoretical work by Denisenkov et al. (2003). For the PDCZ and from He07 respectively He07 extracted the following values as upper limits: f_1=0.01, D_2=10^5cm^{2}s^{-1}, f_2=0.14.

Concerning the bottom of convective envelope during TDU, we chose f_2 to match the mixing profile of IGWs derived by De03, and D_2 to match the maximum of the IGW profile modelling the rapid decay of our mixing coefficient profile through a rapid decay across the convective boundary using a small f_1. In this work we used as default f_1=0.014, D_2=10^{11}cm^{2}s^{-1}, f_2=0.25.

2.2. Comparison with observations

The observation of the surface abundances of the PG1159 objects reveal the He-intershell abundances at late AGB stages, where the amount of the most abundant elements He, C and O are relics of the AGB stellar evolution and diagnostics for CBM during this earlier phase (e.g., Werner et al. 2006).

In Fig. 2 we report the abundances observed for PG1159 stars (Werner et al. 2006). In particular, in the same plot we show the results from model M2.z2m2.he07 as a representative case of our calculations.

In Fig. 3, the [hs/ls] ratio obtained in our models is compared with spectroscopic observations of galactic-disk AGB stars (Abia et al. 2002; Zamora et al. 2009). The results for the stellar models with the same initial mass from the FRUITY database are also shown (Cristallo et al. 2015). The models shown do not include other relevant physics mechanisms such as rotation and magnetic field. In particular our models reproduce the highest [hs/ls] values de-

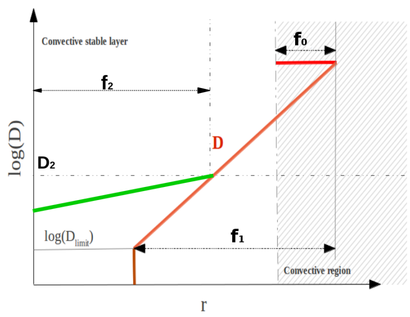

Fig. 1. Schematic description of the double-exponential CBM applied in this work. The red line is the standard overshooting mixing coefficient profile following the single-exponential decay. This profile is dominated by a single 'f_1' parameter which determines the slope of the mixing profile: the lower the 'f' value, the steeper the profile is. In order to take into account IGW, in this work we apply a second, slower, decreasing profile (green line) that becomes more relevant than the first one as soon as the mixing coefficient is equal or lower that a 'D_2' value, the slope of which is determined by the 'f_2' parameter. Check the text for the relation between D and and all the CBM parameters.

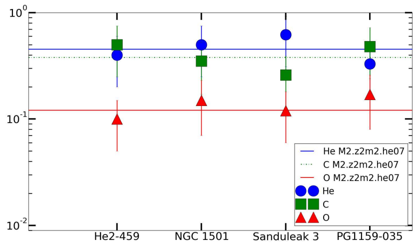

Fig. 2. He, C and O abundances observed for a sample of H-deficient post-AGB stars classified as PG1159 objects: He2-459, NGC1501, Sanduleak3 and PG1159-035. Observations are given by Werner et al. (2006). Also the final intershell abundances from M2.z2m2.he07 are presented.

rived from the observations, and a stochastic process like rotations would lower the final [hs/ls] helping in properly reproducing the observed spread.

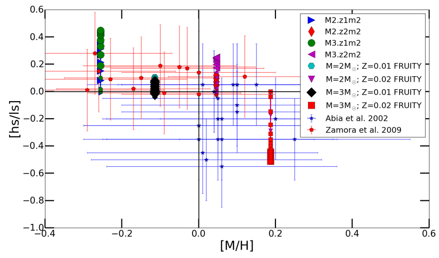

Fig. 3. Comparison of the [hs/ls] vs [M/H] obtained from our models with observational data from Abia et al. (2002) and Zamora et al. (2009). We also report the AGB calculations from the FRUITY database (Cristallo et al. 2015).

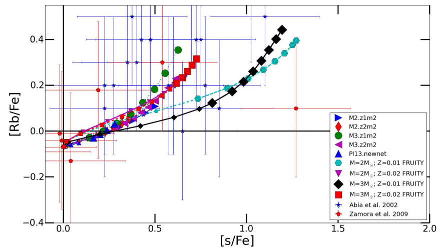

Fig. 4. I report the [Rb/Fe] and [*s*/Fe] ratios obtained from the indicated AGB models, in comparison with a sample of C stars by Abia et al. (2002) and Zamora et al. (2009), and with analogous theoretical AGB models by the FRUITY database (Cristallo et al. 2015). Only stars with [M/H] >-0.3 are considered.

In Fig. 4, we compare our models with spectroscopic observations for [Rb/Fe] and the [s/Fe] ratio, given by the average production at the ls and hs *s*-process neutron-magic peaks. The [s/Fe] ratio is a diagnostic for the *s*-process efficiency, and the [Rb/Fe] ratio increases with the increase of the efficiency of the ^{22}Ne(α,n)^{25}Mg reaction during the TP (e.g., Lambert et al. 1995).

Overall, both sets of models in Fig. 3 are consistent with observations. This is also due to the large observational uncertainties, reported in the figure.

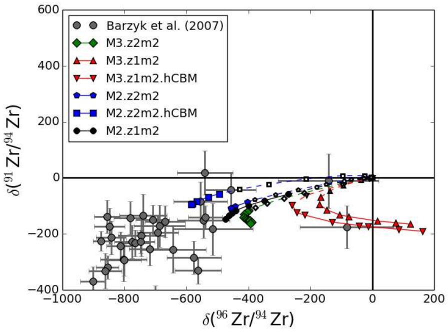

Fig. 5. The evolution of $\delta(^{91}Zr/^{94}Zr)$ and $\delta(^{96}Zr/^{94}Zr)$ ratios in the AGB envelope is shown for our AGB models. Large full markers identified the abundances at each TP once C>O at the surface, while small empty markers identify the occurrence of TPs before the AGB models become C rich. For comparison, the measurements from presolar SiC grain of type mainstream and error bars are reported (Barzyk et al. 2006).

Finally, I compare the results of my stellar calculations with measurements of isotopic abundances in presolar mainstream SiC grains for Zr and Ba. If we look carefully at theoretical evolution curves in Fig. 5, all the models with initial mass equal to 3 $M_\odot$ show a signature of efficient ^{96}Zr production due to the $^{22}Ne(\alpha,n)^{25}Mg$ activation at the bottom of the convective TP, eventually leading to positive δ-values, without therefore explaining the abundances for all the presolar grains.

3. Conclusions

For the first time, the models here study the impact of the following physics ingredients on AGB stellar evolution and nucleosynthesis: the Convective-Boundary-Mixing (CBM) at the bottom of the convective TPs according to Herwig et al. (2007) simulations and the CBM below the TDU driven by Internal-Gravity-Waves (IGW) according to Denisenkov et al. (2003). We have compared our models with different types of observations, including spectroscopic data from Carbon stars and isotopic measurements in presolar mainstream SiC grains. At the end of the AGB evolution we obtain an *s*-process production 0.36 <[*s*/Fe] <0.78 and -0.23 <[hs/ls] <0.45, which is consistent with spectroscopic observations of C-rich AGB stars. Within the mass range considered we do not produce low enough $\delta(^{96}Zr/^{94}Zr)$ ratios as observed. On the other hand, present AGB models are getting much closer to fit the grain data than previous works where the CBM at the bottom of the PDCZ was used, in particular for the ratio $\delta(^{96}Zr/^{94}Zr)$. The main reason of this improvement is due to the new nuclear reaction rates in the Zr region, with a much lower ^{95}Zr neutron capture cross section reducing the production of ^{95}Zr in the convective TPs. I believe that AGB models including rotation (and magnetic field) may also have an important impact in this discussion. At least rotation affects the ^{13}C-pocket history once the ^{13}C-pocket has formed (Piersanti et al. 2013) reducing the neutron exposure and favoring the production of light *s*-isotopes like ^{94}Zr-, eventually reducing the $\delta(^{96}Zr/^{94}Zr)$.

Acknowledgements. NuGrid acknowledges significant support from NSF grants PHY 02-16783 and PHY 09-22648 (Joint Institute for Nuclear Astrophysics, JINA), NSF grant PHY-1430152 (JINA Center for the Evolution of the Elements) and EU MIRG-CT-2006-046520. I acknowledge the support from SNF (Switzerland). NuGrid data is served by Canfar/CADC.

References

Abia, A., et al. 2002, ApJ, 579, 817
Barzyk, J. G., et al. 2006, New Astron. Rev., 50, 587
Cristallo, S., et al. 2015, ApJS, 219, 40
Denisenkov, P., et al. 2003, MNRAS, 340, 722
Gallino, R., et al. 1998, ApJ, 497, 388
Herwig, F., et al. 2005, ARA&A, 43, 435
Herwig, F., et al. 2000, A&A, 360, 952
Herwig, F., et al. 2007, ASP Conf. Ser., 378
Lambert, D. L., et al. 1995, ApJ, 450, 302
Lugaro, M., et al. 2003, ApJ, 593, 486
Piersanti, L., et al. 2013, ApJ, 774, 98
Sterling, N. 2002, ApJ, 578, L55
Straniero, O. 1995, ApJ, 440, L85
Werner, K., et al. 2006, PASP, 118, 183
Sterling, N. 2002, ApJ, 578, L55
Zamora, O. 2009, A&A, 508, 909